Heat Transfer for Turbulent Flow in Rectangular Ducts with Two Heated and Two Unheated Walls

J. L. NOVOTNY, S. T. McCOMAS, E. M. SPARROW, and E. R. G. ECKERT

University of Minnesota, Minneapolis, Minnesota

Many heat exchanger applications require cooling passages with noncircular cross sections. Up to the present time the majority of the experimental and theoretical work on internal turbulent flow and heat transfer has been confined to the circular tube. The circular configuration, besides its technical importance, also lends itself to analysis, and thus it has been extensively investigated.

It has been shown that for certain noncircular geometries the turbulent pressure drop can be predicted from circular-tube relations when the tube diameter is replaced by the hydraulic diameter of the noncircular cross section. Experimental studies (*1*) have revealed that the pressure drop in rectangular ducts with aspect ratios ranging from 1:1 to 10:1 can be predicted in this manner to within 5%. It should be pointed out that this does not hold for all geometries; for example experimental studies (*2, 3*) have shown that the hydraulic-diameter rule can be in error by as much as 20% in small opening-angle triangular ducts. The hydraulic-diameter rule overestimates the pressure drop, with the deviation being inversely proportional to the opening angle. For laminar flows the pressure drop is even more sensitive to the shape of the duct cross section, and the hydraulic diameter does not correlate results for circular and noncircular shapes.

The heat transfer characteristics of noncircular geometries have been investigated to a lesser extent than the flow. An experimental investigation (*2*) of turbulent heat transfer in an electrically heated triangular duct with an opening angle of 11.46 deg. has demonstrated that the hydraulic-diameter rule overestimates the average heat transfer coefficient by as much as a factor of 2. Another important limitation of the hydraulic-diameter concept is that local heat transfer conditions cannot be determined, especially the circumferential variations of wall temperature or wall heat flux. This is a serious limitation, since in certain geometries local temperatures can be considerably higher than those predicted by average results, for instance as in (*2*). Local hot spots such as these can impose serious practical metallurgical and structural limitations. Reference 2 points out an additional interesting aspect of noncircular duct heat transfer, namely that under certain heating conditions the thermal entrance length may greatly exceed that for the circular tube.

Most of the experimental investigations of heat transfer in rectangular ducts fall in the category of boiling burnout tests; however there are a number of papers that report heat transfer results for single-phase flow (*4* through *14*). In some of these investigations the thermal boundary conditions were not well defined, and in many cases insufficient instrumentation was employed to obtain detailed information. Thus it appeared worthwhile to systematically and carefully investigate the heat transfer characteristics of rectangular ducts of different aspect ratios with the particular aim of determining whether the heat transfer is greatly affected by the thermal boundary conditions.

This report presents fully developed heat transfer results for turbulent flow of air in rectangular ducts with aspect ratios of 1:1, 5:1, and 10:1. The heating condition is such that the two longer walls of the rectangle are uniformly heated, while the two shorter walls are unheated. These boundary conditions correspond closely to those found in nuclear reactor applications.

Table 1. Dimensions of Ducts
(all length dimensions in inches)

Nominal aspect ratio	Width a ($\pm$0.005)	Height ($\pm$0.005)	D_h	Length of unheated section	Length of heated section
1:1	0.980	0.980	0.980	47	206
5:1	3.000	0.604	1.00	48	140
10:1	4.000	0.400	0.727	48	132

EXPERIMENTAL APPARATUS

Three rectangular ducts of aspect ratios 1:1, 5:1, and 10:1 were used in the present investigation. All ducts were of the same construction and materials, differing only in dimensions of the cross section and in length. Figure 1 shows the construction details, and Table 1 gives the dimensions of each duct.

An unheated starting length was used to obtain hydrodynamically fully developed flow at the entrance to the heated portion of the duct. Uniform heat generation in the top and bottom walls of the test section was achieved by passing an electric current longitudinally through the duct walls, which were constructed from 0.025 in. thick stainless steel plates. To approach as closely as possible the condition of adiabatic side walls the latter were made of a fabricated board which had a thermal conductivity of 0.15 B.t.u./hr.-ft.-°F. With a view towards preventing leakage of air into or out of the duct the stainless steel walls were backed with a ¼-in. reinforcing layer of an epoxy resin.

After leaving the heated section the air passed through an insulated mixing chamber where the exit bulk temperature was measured. The mass flow rate of the air was measured downstream of a flow straightener which was placed between the mixing chamber and the flow measuring device.

The entire duct was mounted in the center of a box of cross-sectional dimensions 18 by 18 in. which extended the entire length of the duct. The box was filled with insulation which

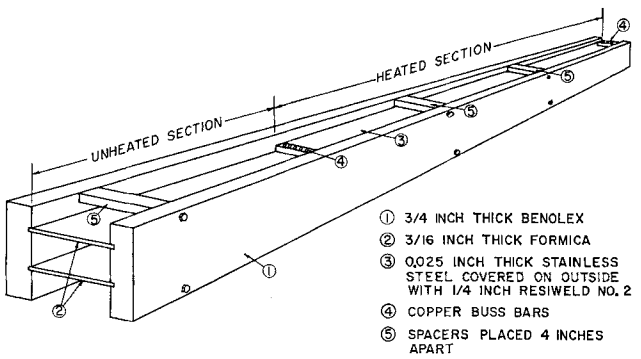

Fig. 1. Schematic of rectangular duct.

has an effective thermal conductivity of approximately 0.0142 B.t.u./hr.-ft.-°F. at a temperature of 150°F.

A detailed description of materials and procedures used in fabricating the ducts is available (*15*).

MEASUREMENTS AND DATA REDUCTION

The essential quantities which were measured in this investigation included the entering and exit air temperatures, wall temperatures, air flow rate, static pressure, and the electrical power input to the duct. The following paragraphs discuss the accuracy of these measurements and how they are used to determine Nusselt numbers for the rectangular ducts.

All thermocouples used in the investigation were taken from calibrated rolls of 36 gauge iron-constantan thermocouple wire. The thermocouple outputs were read with a self-balancing potentiometer which had a calibrated accuracy of ± 2 μv. The temperatures of the heated duct walls were measured by thermocouples attached with copper oxide to the outer surfaces of both of the stainless steel plates. The temperature drop across the thickness of the steel wall was found by computation to be negligible. The wall thermocouples, which ranged in number from 165 to 257 depending on the duct size, were distributed across the span of the heated plates at various longitudinal positions.

The temperature of the air entering the duct was measured by three thermocouples placed in the air stream at the inlet to the unheated starting section. The bulk air temperature at the exit of the test section was measured in a well insulated mixing chamber which caused several reversals in flow direction by means of baffles. The bulk temperature measurement was made by a seven-junction averaging thermocouple situated at the exit of the chamber. Several additional thermocouples were located at various positions in the mixing chamber to check for temperature uniformity within the chamber. The absence of significant temperature variations indicated a negligible heat loss.

A flat-plate orifice was used for the measurement of the lower air flow rates and a Venturi for the higher rates. Both of these instruments were fabricated in accordance with the American Society of Mechanical Engineers Power Test Code specifications and were additionally checked against a calibrated flow nozzle. The scatter in the calibration data suggested an uncertainty in the mass flow measurement of approximately 1%.

The power dissipation in the duct was determined by measuring the total current through the two stainless steel walls and the voltage drop across the duct. Current measurements were made with an ammeter in conjunction with a current transformer, the combined accuracy being ¼% of full scale. The voltage drop was measured with a voltmeter with an accuracy of ½% of full scale. To check the power factor the power input was additionally determined by a wattmeter with an accuracy of ½% of full scale.

A further discussion of measurement techniques and instrumentation is available in reference *15*.

The following equation was used to calculate the rate of heat transfer Q from the stainless steel walls to the air flowing through a unit length of duct:

$$Q = mc_p \frac{dT_b}{dz} - (Q_s - Q_o) \qquad (1)$$

The rate of heat transferred to the air in the duct from both the heated and the unheated walls is given by the first term on the right side of Equation (1). The quantity $(Q_s - Q_o)$ represents the heat transfer from the unheated sidewalls to the air. The increase of the bulk temperature per unit length, dT_b/dz, was obtained under the assumption that the bulk temperature varies linearly between the measured temperatures at the entrance and exit cross sections.

The term Q_s denotes the heat which flows by conduction from the heated duct walls into the unheated side walls per unit length. This quantity was obtained from a plot of the wall temperature distribution across the span of the stainless steel walls. The span-by-span temperature gradient at the point of contact between the steel walls and the side walls was determined from this diagram. With this gradient and with the measured thermal conductivity of the stainless steel the heat flux leaving the wall was calculated from Fourier's heat conduction equation. The contribution of Q_s to the heat flux Q was largest at low mass flow rates. At its very maximum it amounted to 22% of the heat generation for the 1:1 aspect ratio duct at low Reynolds numbers. In the other ducts Q_s never exceeded 10% of the electrical power. The span-by-span heat conduction through the Resiweld backing could not be determined from the experiments. It was computed that the span-by-span conductance of the backing was on the order of one tenth of that of the stainless steel, and on this basis the contribution of the backing was neglected. The contact resistance at the point of attachment to the sidewalls could not be estimated.

Of the heat Q_s conducted from the heated walls to the unheated side walls a portion Q_o passes through the surrounding insulation to the room. The remainder $(Q_s - Q_o)$ is transferred to the air flowing in the duct. The heat loss Q_o from the unheated side walls was determined by prorating the overall heat loss in accordance with the internal surface area of the duct. The overall heat loss was computed as the difference between the electric power dissipated in the two heated walls and the enthalpy rise of the air flowing through the duct. The quantity Q_o was always less than 1.5% of the power input, except for the 1:1 duct; in the latter Q_o was 6%. The overall heat loss ranged from 1 to 12% of the power input.

The next quantity needed for the computation of the span-by-span average heat transfer coefficient is the wall-to-bulk temperature difference $\overline{(T_w - T_b)}$ averaged across the heated walls. First the length of duct beyond which fully developed thermal conditions prevailed was determined; plots were made of the longitudinal temperature distribution along both heated walls. On these plots a straight line was drawn connecting the entering and exit bulk temperatures of the air. The fully developed regime is assumed to be achieved when the slopes of the wall and bulk temperature curves become equal. Next, with data at a number of cross sections in the fully developed region utilized, a plot was made of the span-by-span distribution of the wall-to-bulk temperature difference. This plot was then used to determine the average difference between the wall and the bulk temperature.

The heat transfer coefficient $\bar{h}$ for fully developed conditions is then defined by

$$Q = \bar{h}(2a)\ \overline{(T_w - T_b)} \qquad (2)$$

where Q is the heat flux per unit duct length and a is the width (that is span-by-span dimension) of the heated wall. The Nusselt number is formed by using the wetted hydraulic diameter D_h as the characteristic dimension in accordance with

$$N_{Nu} = \frac{\bar{h} D_h}{k} \qquad (3)$$

The thermal conductivity k was evaluated at the average bulk temperature of the air between the inlet and the exit of the duct. It should be emphasized that the entire wetted perimeter is utilized in computing D_h.

The span-by-span variation of the heat transfer in the thermally fully developed regime was also calculated. For

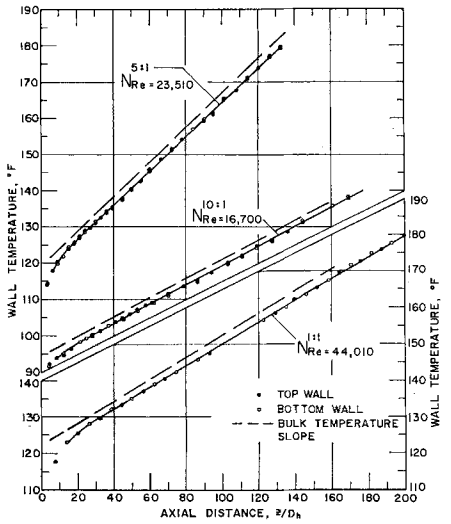

Fig. 2. Representative axial distribution of center-span temperature along heated walls.

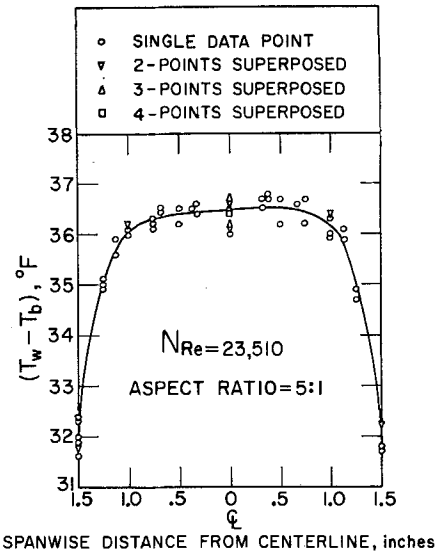

Fig. 3. Representative span-by-span temperature distribution across heated walls, 5:1 duct.

the purposes of the calculation the duct wall was subdivided along its span into ¼-in. segments, and an energy balance was applied to each segment. The net heat loss by span-by-span conduction was determined for each segment from the span-by-span distribution of the wall temperature. There is no net loss by longitudinal conduction for fully developed conditions. Since the span-by-span variation in temperature was small compared with the difference between the wall and room-ambient temperatures, the heat loss to the surroundings was prorated uniformly across the duct width. The heat transferred from each segment to the flowing air was then calculated by subtracting the loss to the surroundings and the heat loss by span-by-span conduction from the local* heat generation. The local heat transfer coefficient was then computed as the ratio of the local heat flux to the air to the local wall-to-bulk temperature difference. The aforementioned span-by-span heat transfer calculations were carried out for the 5:1 and 10:1 ducts. The relatively narrow width of the 1:1 duct made such a determination impractical.

EXPERIMENTAL RESULTS AND CONCLUSIONS

Heat transfer measurements were made in each of the three ducts for a wide range of air flow rates. A summary of the experimental data is given in reference *15*. The Reynolds number range of the runs was approximately 10,000 to 140,000 except the 10:1 duct. Owing to an overheating accident which destroyed the 10:1 duct beyond repair, the investigated Reynolds number range is smaller ($< 70{,}000$) for this duct than for the remaining two ducts. The lower end of the Reynolds number range lies above the limit at which free convection effects are noticeable, while the upper end of the range lies below the limit of significant compressibility effects. Because of space limitations local results will be given in detail only for one representative run for each aspect ratio. The local results for other Reynolds numbers do not differ greatly from those presented.

The longitudinal distribution of the temperature measured at the center line of each heated wall is presented in Figure 2 for the 1:1, 5:1, and 10:1 ducts. Also shown on this figure is a dashed line representing the slope of the bulk temperature rise. The Reynolds number which characterizes each temperature distribution is based on average bulk properties. The fully developed heat transfer condition for longitudinally uniform heat flux is assumed to be attained when the wall temperature curve becomes linear and parallel to the corresponding bulk temperature curve. It can be seen from the figures that this condition is actually achieved. This finding applies no matter whether one chooses the center line or any other span-by-span location for the wall-temperature plot. Thus there appears to be no clear influence of the side walls on the thermal development. The thermal entrance length appears to be less than 30 hydraulic diameters for all aspect ratios and Reynolds numbers of this investigation. Because of the asymptotic nature of the thermal development and of the scatter of the data it was not possible to assign a more precise value to the entrance length.

Representative span-by-span temperature profiles for the 5:1 and 10:1 aspect ratio ducts are shown in Figures 3 and 4, respectively. Corresponding data for the 1:1 duct are omitted for reasons already discussed. The ordinate of the figures is the difference between the local wall temperature and the bulk temperature. The plotted points include data for a number of axial positions in the fully developed region. The curve which was passed through the data appeared to be the best fit. It is seen from Figure 4 that there are definite hot spots near the corners of the 10:1 duct; however no corresponding hot spots are evident for the 5:1 duct, Figure 3. One would expect that if

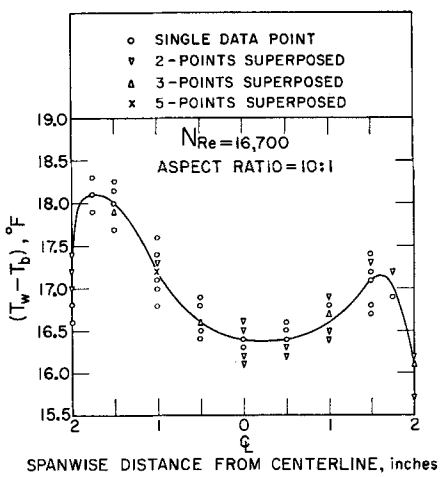

Fig. 4. Representative span-by-span temperature distribution across heated walls, 10:1 duct.

* The heat generation rate for the 10:1 duct varied in span-by-span direction by 5% owing to a corresponding linear variation in wall thickness.

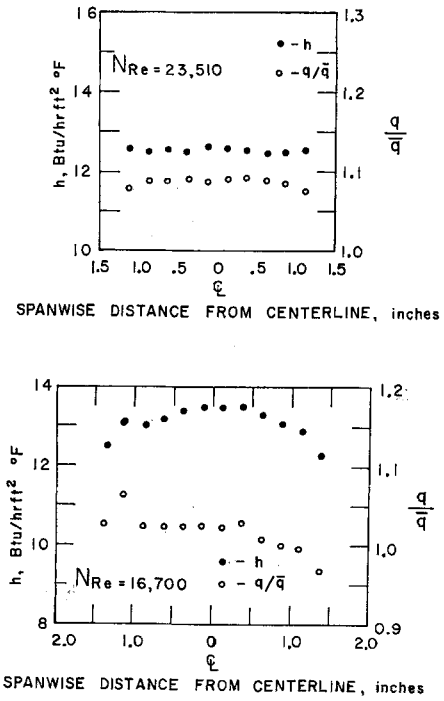

Fig. 5. Representative span-by-span distribution of local heat flux and local heat transfer coefficient across heated walls. (Top) *a.* 5:1 aspect ratio. (Bottom) *b.* 10:1 aspect ratio.

the side walls were truly adiabatic, hot spots would exist in the corners of both ducts since the local heat transfer coefficient will be smaller near the corners. The fact that the temperature difference $(T_w - T_b)$ decreases near the corners is due to the conduction of heat into the side walls. This conduction is sufficient to suppress the hot spots in the 5:1 duct. The asymmetry of the temperature profile for the 10:1 duct is caused by a slight linear variation in wall thickness (about 5% across the section) which induces a somewhat nonuniform internal heat generation. As has already been noted, account of this is taken in the computation of the local heat transfer coefficient.

The span-by-span distribution of the local heat flux from the heated walls to the air is shown in Figure 5 for the 5:1 and 10:1 ducts. The data exhibit some scatter; however it is seen from the figures that the uniform heat flux condition is approximated except near the edges where conduction to the side walls reduces the local heat flux. Additionally the span-by-span distribution of the local fully developed heat transfer coefficient is plotted in Figure 5. These results represent the ratio of the local heat flux, also shown in Figure 5, to the corresponding local temperature difference given in Figures 3 and 4. These distributions of h are somewhat influenced by the span-by-span conduction into the side walls.

The span-by-span averaged fully developed Nusselt numbers for the three aspect-ratio ducts are shown in Figure 6 as a function of the average bulk Reynolds number. The characteristic dimension in both the Nusselt number and the Reynolds number is the hydraulic diameter (see Table 1) based on the entire wetted perimeter. The present results are compared with the circular-tube empirical correlation of Colburn (*16*) as well as with the analytical results of Siegel and Sparrow (*18*) for the circular tube and Sparrow and Lin (*17*) for the parallel-plate channel. Both analytical studies were carried out for the case of uniform wall heat flux.

The analysis for the parallel-plate channel yields Nusselt numbers which are approximately 5% larger than the results of the circular-tube analysis at a Reynolds number of 10^5 and are approximately 10% higher at a Reynolds number of 10^4. The experimentally determined Nusselt numbers are, apart from some scatter, bracketed by the results of the two analyses. The experimental results for the square duct appear to lie slightly higher than the results for the ducts with rectangular cross section. Additionally Figure 6 indicates that the empirically based Colburn correlation of circular-tube data, which is frequently used for engineering calculations, lies somewhat higher than the experimental data, especially at the higher Reynolds numbers. It is worthwhile noting that the greatest uncertainty in both theory and experiment occurs at the lowest Reynolds numbers. It may be observed that apparent good correlation among the present data is achieved with a hydraulic diameter based on the entire wetted perimeter (Figure 6).

ACKNOWLEDGMENT

The authors wish to acknowledge the contributions of Dr. J. P. Hartnett who initiated this study and of S. H. Lin, L. E. Anderson, J. R. Lloyd, and Krishnamachar Sreenivasan who assisted in its execution. The fabrication of the rectangular ducts was carried out by C. R. Retz. The support of the U.S. Atomic Energy Commission under Contract No. AT (11-1)-659 is gratefully acknowledged.

NOTATION

S = cross-sectional area of duct
a = width of heated wall
c_p = specific heat at constant pressure
D_h = entire wetted hydraulic diameter, $4S/L$
h = local heat transfer coefficient
$\overline{h}$ = average heat transfer coefficients, Equations (2) and (4)
k = thermal conductivity
L = wetted perimeter of duct
m = mass rate of air flow
N_{Nu} = average Nusselt number, $\overline{h}D_h/k$
N_{Pr} = Prandtl number, $\mu c_p/k$
Q = heat transfer rate per unit length from heated wall to air
Q_o = heat loss per unit length from unheated side walls
Q_s = heat conducted per unit length from heated walls to unheated side walls
$\overline{q}$ = peripherally averaged heat flux rate
N_{Re} = average bulk Reynolds number, $\overline{w}D_h/\nu$
T = temperature

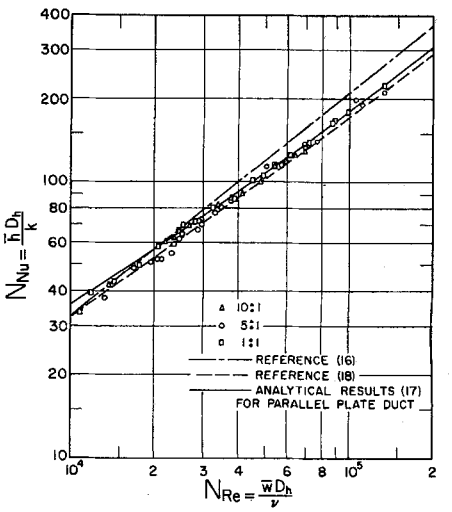

Fig. 6. Fully developed Nusselt number results.

T_w = wall temperature
T_b = bulk temperature
$\overline{w}$ = mean velocity
z = axial coordinate
μ = absolute viscosity
ν = kinematic viscosity

LITERATURE CITED

1. Hartnett, J. P., J. C. Y. Koh, and S. T. McComas, *J. Heat Transfer*, **84**, 82 (1962).
2. Eckert, E. R. G., and T. F. Irvine, Jr., *ibid.*, **82**, 125 (1960).
3. Carlson, L. W., and T. F. Irvine, Jr., *ibid.*, **83**, 441 (1961).
4. Cope, W. F., Technical Reports of Aeronautical Research Committee, Great Britain, R and M No. 1359, 384 (1930).
5. Bailey, A., and W. F. Cope, Technical Reports of Aeronautical Research Committee, Great Britain, R and M No. 1560, 199 (1933).
6. Washington, L., and W. M. Mark, *Ind. Eng. Chem.*, **29**, 337 (1937).
7. Kays, W. M., and A. L. London, *Trans. Am. Soc. Mech. Engrs.*, **74**, 1179 (1952).
8. Lowdermilk, W. H., W. F. Weiland, Jr., and J. N. B. Livingood, *Natl. Advisory Comm. Aeronaut. RM E53J07* (1954).
9. Levy, S., R. A. Fuller, and R. O. Niemi, *J. Heat Transfer*, **81**, 129 (1959).
10. Roarty, J. D., and N. C. Sher, Atomic Power Division, Westinghouse Corp., WAPD-TH-217 (July 17, 1956).
11. Lancet, R. T., *J. Heat Transfer*, **81**, 168 (1959).
12. Shlykov, Yu. P., *Atomnaya Energ.*, **8**, 144 (February, 1960).
13. Heineman, J. B., "An Experimental Investigation of Heat Transfer to Superheated Steam in Round and Rectangular Channels," Argonne National Lab., Illinois (September, 1960).
14. Foltz, H. L., "Heat Transfer and Pressure Drop in a Vertical Square Tube." Goodyear Atomic Corp., Portsmouth, Ohio, GAT-236 (July, 1958).
15. Novotny, J. L., S. T. McComas, E. M. Sparrow, and E. R. G. Eckert, *Heat Transfer Lab. Tech. Rept. No. 52*, Univ. of Minnesota, Minneapolis, Minnesota (1963).
16. Colburn, A. P., E. M. Schoenborn, and C. S. Sietton, *Natl. Advisory Comm. Aeronaut. Rept. No. UD-NI* (1945); *TN 1488* (1948).
17. Sparrow, E. M., and S. H. Lin, *Int. J. Heat and Mass Transfer*, **6**, 248 (1963).
18. Siegel, R., and E. M. Sparrow, *J. Heat Transfer*, **82**, 152 (1960).
19. Deissler, R. C., and M. F. Taylor, *Natl. Aeronaut. Space Administration TR R-31* (1959).
20. Eckert, E. R. G., and R. M. Drake, "Heat and Mass Transfer," 2 ed., McGraw-Hill, New York (1959).
21. Martinelli, R. C., *Trans. Am. Soc. Mech. Engrs.*, **69**, 947 (1947).

Manuscript received September 6, 1963; revision received December 5, 1963; paper accepted December 5, 1963.

APPENDIX

Heat Transfer Analysis for Peripherally-Uniform Wall Temperature

Deissler and Taylor (*19*) have proposed a method for calculating the velocity and temperature fields, along with the pressure drop and heat transfer, for turbulent flow through noncircular geometries. The calculations, which are iterative, are based on the assumption that the universal velocity and temperature profiles for circular tubes are valid along perpendiculars to the wall. Following the original work by Deissler and Taylor for square and equilateral triangular ducts the method has been extended to other geometries. References *2* and *3* present pressure drop and heat transfer results for isosceles triangular ducts, and reference *1* reports the pressure drop in rectangular ducts of various aspect ratios. Fully developed heat transfer results for various aspect ratio rectangular ducts with the boundary condition of uniform axial heat flux and uniform peripheral wall temperature will be given here. This peripheral boundary condition differs from that of the foregoing experiments, and hence the analytical results are intended to supplement the measurements.

The velocity distribution which is needed as input to the heat transfer analysis has already been computed by the Deissler-Taylor method in (*1*). To facilitate the heat transfer analysis it is assumed that the temperature field in any cross section is similar to the velocity field. It follows that the isotherms are coincident with the velocity contours; correspondingly the temperature gradient lines (the gradient lines are normal to the isotherms) are coincident with the velocity gradient lines which have already been determined in (*1*). This assumption greatly simplifies the calculation inasmuch as it eliminates the iteration process which is normally involved in the Deissler-Taylor method and is supported by the fact that the Prandtl number for air is nearly 1.

Only a brief outline of the heat transfer analysis can be given here owing to space limitations; a detailed description can be found in (*15*). In essence the analysis is carried out by subdividing the duct cross section into a number of control volumes each bounded by two temperature gradient lines (that is adiabatics) and a segment of the wall. The universal temperature profile T^+ vs. y^+ (see for instance references *15*, *20*, or *21*) is assumed to apply along a perpendicular constructed at the midpoint of each wall segment. With the aid of the relationship between y^+ and the physical distance which is available from reference *1* one can construct the T^+ distribution throughout the entire cross section.

Next a cross-sectional, average heat transfer coefficient and Nusselt number may be defined as

$$N_{Nu} = \overline{h}D_h/K, \quad \overline{h} = \overline{q}/(T_w - T_b) \qquad (4)$$

The wall-to-bulk temperature difference may be represented as an integral of the velocity and temperature profiles over the cross section. In addition the peripherally averaged heat flux $\overline{q}$ can be related to the local heat flux passing from each wall segment into the air. From these operations it follows that the Nusselt number is calculable by integrating over the cross section a quantity involving the universal temperature and velocity profiles along with geometrical parameters which are related to the control volumes.

The average fully developed Nusselt numbers which were calculated in this manner are presented in Figure 7 for aspect ratios ranging from 1:1 to ∞:1. The results show a definite effect of the aspect ratio in that the Nusselt number increases monotonically as the aspect ratio increases. This trend is therefore the same as the one which was found experimentally for the 5:1 and 10:1 ducts in the lower range of Reynolds numbers, see Figure 6. However the 1:1 aspect ratio data do not fit into this pattern. In appraising these findings it should be noted that the peripheral boundary conditions of experiment and analysis are not the same. In addition the data for the 1:1 aspect ratio duct are prone to greater uncertainty owing to the larger side-by-side conduction. Finally the analysis assumes that the turbulent diffusivity is isotropic; experiments in a triangular duct (*2*) suggest that such is not actually the case.

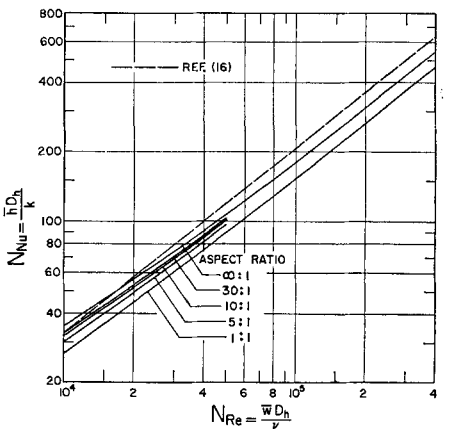

Fig. 7. Fully developed Nusselt numbers predicted from Deissler-Taylor calculation method.